Observing fracture lineaments with Euler curvature

Satinder Chopra, *Arcis Seismic Solutions, TGS, Calgary, Alberta, Canada*
Kurt J. Marfurt, *University of Oklahoma, Norman, Oklahoma, USA*

Abstract

In the last several years, seismic-curvature attributes have been shown to be very useful in delineation of folds, flexures, and faults. Although many curvature measures have been introduced, the most-positive and most-negative principal curvatures (k_1 and k_2) are found to be the most useful. All other curvature measures can be derived from the two principal curvatures. For example, the components of apparent curvature projected parallel to the dip azimuth and strike of a dipping plane are useful in given tectonic and stress settings. Euler curvature is a generalization of the dip and strike components of curvature in any user-defined direction, as applied to the interpretation of surface-seismic data. This attribute is useful for interpretation of lineament features in desired azimuthal directions, for example, perpendicular to the minimum horizontal stress. If a given azimuth is known or hypothesized to be correlated with open fractures or if a given azimuth can be correlated with enhanced production or effective horizontal drilling, a Euler-curvature intensity volume can be generated for that azimuth, thereby high-grading potential sweet spots.

Introduction

In his seminal paper, Roberts (2001) describes 12 types of surface-based attribute measures. Many of those attributes have been extended to volume computations and have been implemented on interpretation workstations. Of those different curvature attributes, the most-positive and most-negative principal curvatures (k_1 and k_2) are the most popular.

Not only are k_1 and k_2 intuitively easy to understand, they also provide more continuous maps of faults and flexures than the maximum and minimum curvatures. Mathematically, k_{max} is the eigenvalue and φ_{max} is the azimuth of the eigenvector that best represents the deformation of a 2D surface in a 3D volume; k_{min} and φ_{min} represent the less intense deformation in the orthogonal direction. For this reason, k_{max} and k_{min} can rapidly change sign at fault and flexure intersections.

We also prefer to use strike ψ rather than the perpendicular azimuth φ because it implies clearly that curvature has a periodicity of 180°. Although several other practitioners have used other attributes such as the mean curvature, Gaussian curvature, and shape index, some other curvature attributes which Roberts (2001) introduces warrant investigation and form the motivation for the present work. One of them is Euler curvature.

Discontinuity attributes are used routinely to map fault traces and fault damage zones. Subsequent image-processing algorithms can then be used to estimate the strike of the discontinuities. Although this method generally works well, strong anomalies associated with faults that have large displacement will often mask weaker anomalies so that only the dominant fracture lineaments are mapped.

Image-processing filters can provide direct user control on discontinuity enhancement. Singh et al. (2008) use an ant-tracking algorithm to enhance discontinuities associated with hypothesized fracture corridors that have a specific azimuthal orientation, which are then merged into a single 3D volume of fracture clusters. Ant tracking is a proprietary iterative scheme that progressively tries to connect adjacent zones of low coherence that have been filtered to eliminate horizontal features associated with stratigraphy. Although ant-tracking algorithms also can be applied to most-positive and most-negative principal curvature lineaments, a more natural method is to compute a suite of Euler curvatures.

Definition and workflow

In this paper, we describe the application of volumetric Euler curvature to 3D seismic data volumes. Euler curvature can be thought of as apparent curvature perpendicular to a given strike direction. If (k_1, ψ_1) and (k_2, ψ_2) represent the magnitude and strike of the most-positive and most-negative principal curvatures, then the Euler curvature at an angle ψ in the dipping plane tangent to the analysis point (where ψ_1 and ψ_2 are orthogonal) is given as

$$k_e(\psi) = k_1\cos^2(\psi - \psi_2) + k_2\sin^2(\psi - \psi_2). \qquad (1)$$

Because reflector dip magnitude and azimuth can vary considerably across a seismic survey, it is more useful to equally sample azimuths of Euler curvature on the horizontal x-y-plane, project the lines onto the local dipping plane of the reflector, and implement equation 1. The flow diagram in Figure 1 explains the method for computing Euler curvature.
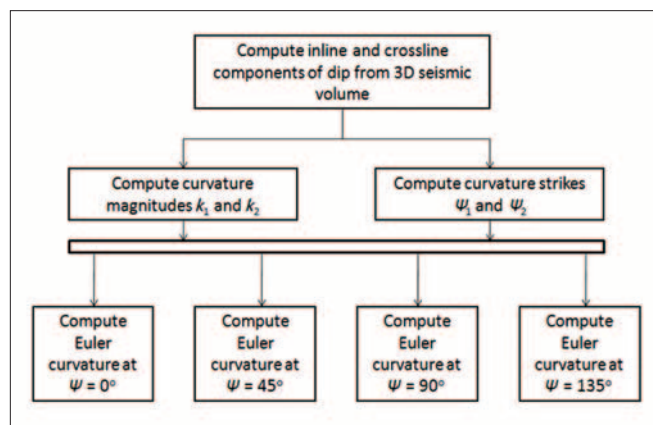

Figure 1. *Flow diagram showing the computation of Euler curvature.*

Applications

Mapping the intensity of a given fracture set has been a major objective of reflection seismologists. The most successful work has used attributes computed by azimuthally limited prestack data volumes. Chopra et al. (2000) show how coherence attributes computed from azimuthally restricted seismic volumes can enhance subtle features hidden or blurred in the all-azimuth volume. Vector-tile and other migration-sorting techniques are now the method of choice for conventional P-wave and converted-wave prestack imaging (e.g., Jianming et al., 2009) and allow prediction of fracture strike and intensity.

Curvature, acoustic impedance, and coherence are currently the most effective attributes used to predict fractures in the poststack world (e.g., Hunt et al., 2010). Rather than map the intensity of the strongest attribute lineaments, Singh et al. (2008) use an image-processing (ant-tracking) algorithm to enhance curvature and coherence lineaments that were parallel to the strike of open fractures, at an angle of about 45° to the strike of the strongest lineaments.
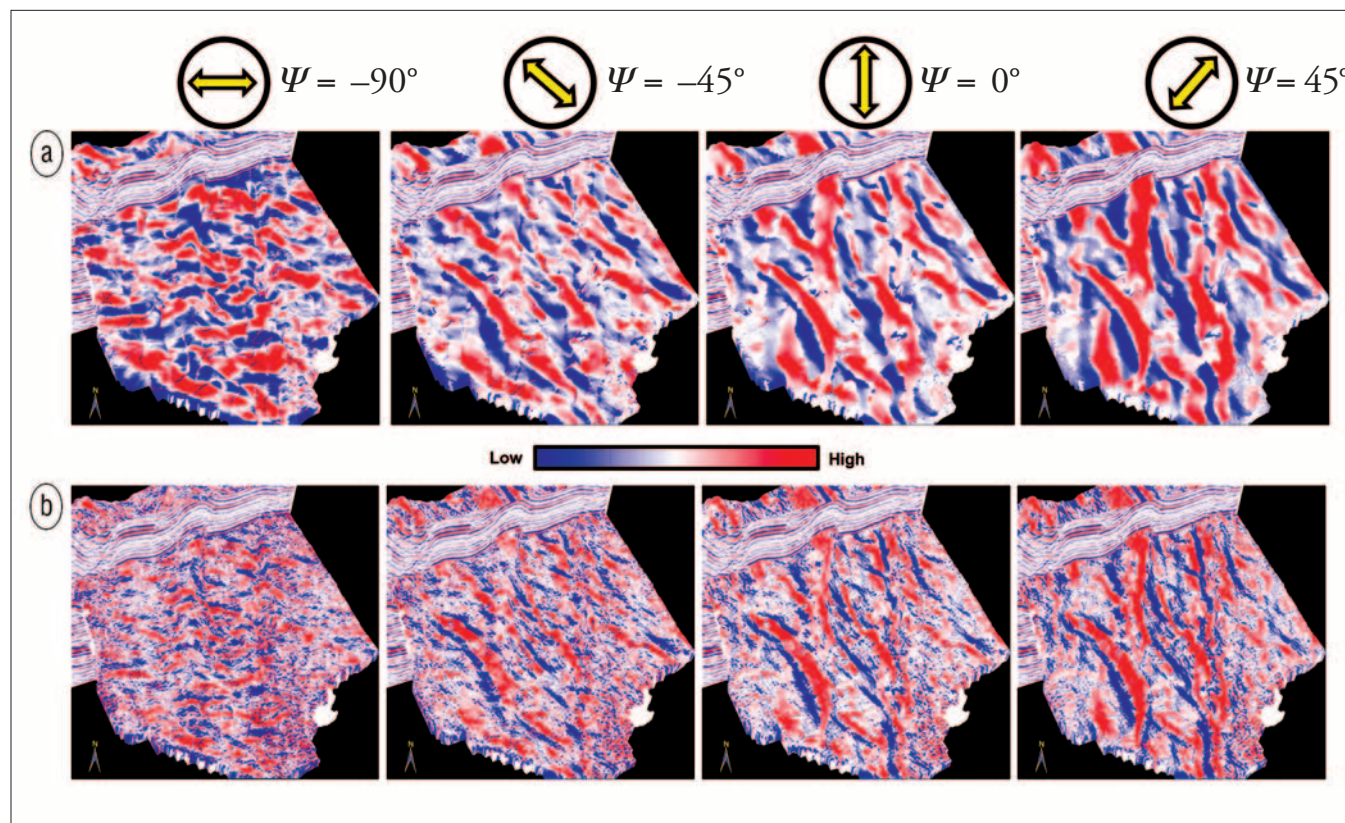

Figure 2. *3D chair views of the correlation of vertical slice through seismic amplitude with the strat-cube through a suite of (a) long-wavelength and (b) short-wavelength Euler-curvature attribute volumes. The term* strat-cube *used here refers to a slab of attribute data about a given horizon and so is equivalent to a suite of stratal slices For each strike, the orthogonal lineaments appear more well defined than those in other directions. 100 km² of data are shown on the curvature displays.*
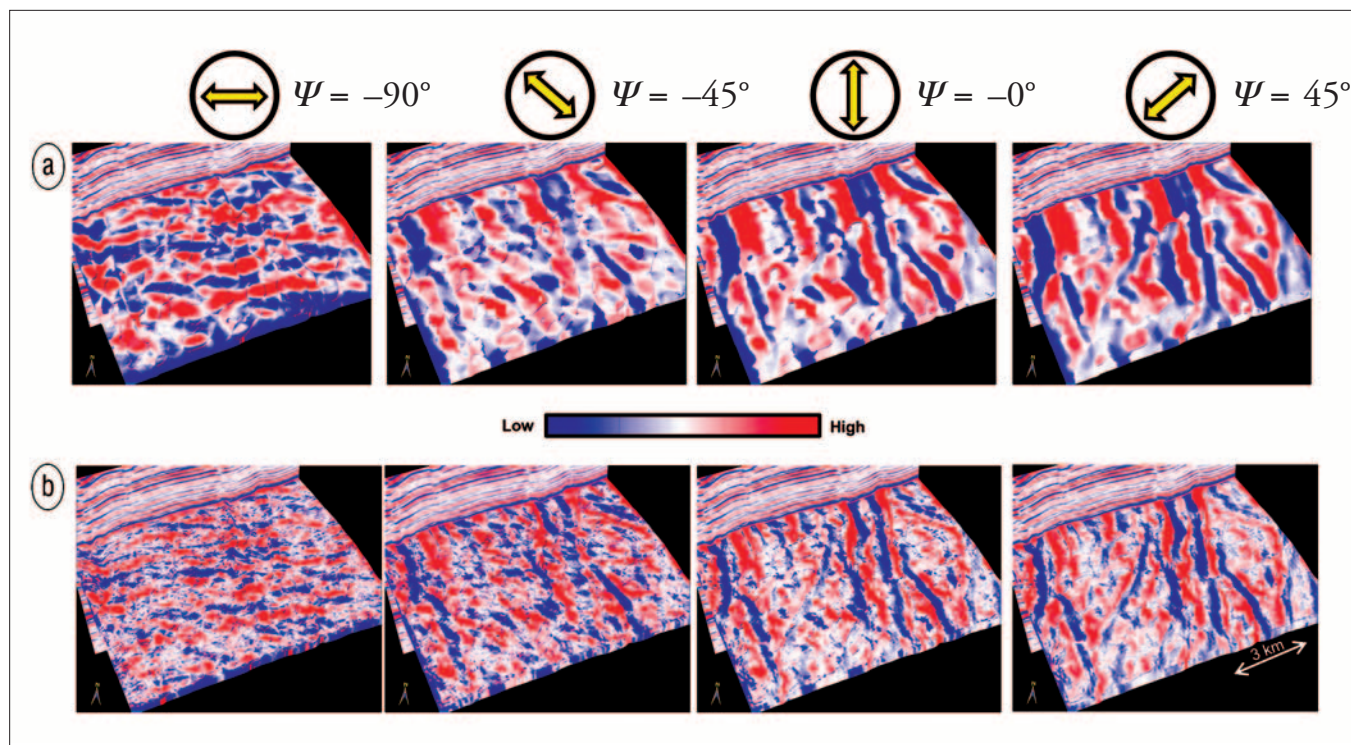
Figure 3. 3D chair views of the correlation of a vertical slice through seismic amplitude with a suite of strat-cubes through (a) long-wavelength and (b) short-wavelength Euler-curvature attribute volumes. For each azimuth strike, the lineaments appear more well defined than those in other directions.

Henning et al. (2010) use related technology to azimuthally filter lineaments in the Eagle Ford Formation of southern Texas. They then compute rms maps of each azimuthally limited volume that can be correlated to production. Guo et al. (2010) hypothesize that each azimuthally limited attribute volume computed from k_1 and ψ_1 corresponds to open fractures. Each volume is then correlated to production to validate or reject the hypothesis.

Daber and Boe (2010) describe the use of what they refer to as azimuthal curvature (described here as Euler curvature following Roberts' definition) for reducing noise in a poststack curvature volume. Daber and Boe (2010) show that if the azimuthal direction is parallel to the inline direction, then the curvature computation is relatively insensitive to the crossline acquisition noise.

We describe here the application of Euler curvature to two 3D seismic volumes from northeastern British Columbia, Canada. We propose an interactive workflow, much as we do in generating a suite of shaded relief maps on which we display apparent dip rather than apparent (Euler) curvature.

Figure 2 shows 3D chair-view displays for Euler curvature for strikes of −90°, −45°, 0°, and +45°. Figure 2a displays the long-wavelength version, and Figure 2b displays the short-wavelength version. Notice that for $\psi = -90°$ lineaments in the east-west direction seem to stand out. For $\psi = -45°$, the lineaments that are almost northwest-southeast are seen as pronounced. Similarly, for $\psi = 0°$, the roughly north-south events stand out, and for $\psi = +45°$, the events slightly inclined to the vertical are more well defined. The same description to

the short-wavelength displays that show more lineament detail and resolution than the long-wavelength display.

Figure 3 shows similar 3D chair-view displays. Again, notice the lineaments becoming pronounced for particular azimuth directions.

The fact that the Euler-curvature displays furnish greater lineament detail can be gauged from Figure 4, in which we show stratal slices from four Euler-curvature orientations and compare them with an equivalent coherence display. Although the dominant discontinuity direction is north-south, there are some discontinuities along other inclinations as well. A good deal more lineament detail is seen in the displays for $\psi = -45°$, $\psi = 0°$, and $\psi = +45°$. Not much is seen in the east-west direction because not much of the coherence stratal slice is shown in that orientation.

There are obvious advantages to running Euler curvature on poststack seismic volumes because azimuth directions can be chosen carefully to highlight lineaments in the directions known through image logs or production data to better correlate to open fractures. That does not entail the processing of azimuth-restricted volumes (usually three or four) all the way to migration and then passing them through coherence/curvature computation.

Conclusions

Euler curvature conducted in desired azimuthal directions provides a quantitative estimate of deformation in a user-defined direction that then could be correlated to borehole, microseismic, and production measurements. Depending on the seismic data quality and the desired level of detail, one can use

long- or short-wavelength computations. Long-wavelength Euler curvature shows broader flexures and folds, and short-wavelength Euler curvature often shows discrete fracture lineaments. **TLE**

References

Chopra, S., V. Sudhakar, G. Larsen, and H. Leong, 2000, Azimuth based coherence for detecting faults and fractures: World Oil, **21**, September, 57–62.

Daber, R. E., and T. H. Boe, 2010, Using azimuthal curvature as a method for reducing noise in poststack curvature volumes: 72nd Conference and Exhibition, EAGE, Extended Abstracts, D024.

Guo, Y., K. Zhang, and K. J. Marfurt, 2010, Seismic attribute illumination of Woodford Shale faults and fractures, Arkoma Basin, OK: 80th Annual International Meeting, SEG, Expanded Abstracts, 1372–1376, http://dx.doi.org/10.1190/1.3513097.

Henning, A. T., R. Martin, G. Paton, and R. Kelvin, 2010, Data conditioning and seismic attribute analysis in the Eagle Ford Shale Play: Examples from Sinor Ranch, Live Oak County, Texas: 80th Annual International Meeting, SEG, Expanded Abstracts, 1297–1301, http://dx.doi.org/10.1190/1.3513081.

Hunt, L., S. Reynolds, T. Brown, S. Hadley, J. Downton, and S. Chopra, 2010, Quantitative estimate of fracture density variations in the Nordegg with azimuthal AVO and curvature: A case study: The Leading Edge, **29**, no. 9, 1122–1137, http://dx.doi.org/10.1190/1.3485773.

Jianming, T., H. Yue, X. Xiangrong, J. Tinnin, and J. Hallin, 2009, Application of converted-wave 3D/3-C data for fracture detection in a deep tight-gas reservoir: The Leading Edge, **28**, no. 7, 826–837, http://dx.doi.org/10.1190/1.3167785.

Roberts, A., 2001, Curvature attributes and their application to 3D interpreted horizons: First Break, **19**, 85–99.

Singh, S. K., H. Abu-Habbiel, B. Khan, M. Akbar, A. Etchecopar, and B. Montaron, 2008, Mapping fracture corridors in naturally fractured reservoirs: An example from Middle East carbonates: First Break, **26**, 109–113.
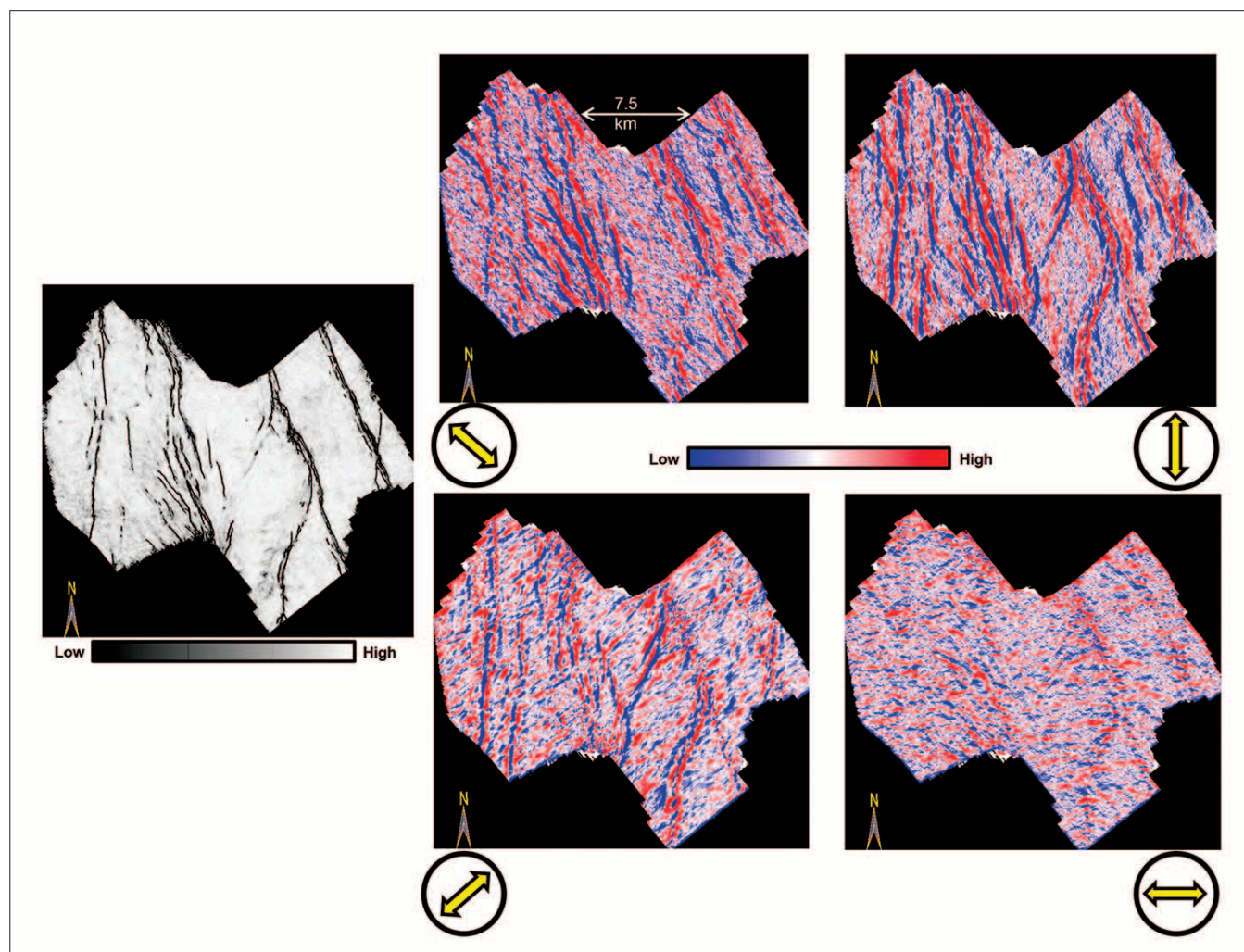
Corresponding author: SChopra@arcis.com

Figure 4. *Stratal displays from Euler-curvature attribute volumes (long-wavelength) run at different strikes, as indicated. For each strike, the lineaments appear more well defined than those in other directions, and lineament detail on those individual displays is more pronounced than on the coherence display.*